frontiers in Immunology

ORIGINAL RESEARCH
published: 29 April 2021
doi: 10.3389/fimmu.2021.648064

Role of Tonsillar Chronic Inflammation and Commensal Bacteria in the Pathogenesis of Pediatric OSA

*Lindybeth Sarmiento Varón[1], Javier De Rosa[1], Raquel Rodriguez[1,2], Pablo M. Fernández[1,3], L. Ariel Billordo[1], Plácida Baz[1], Gladys Beccaglia[4], Nicolás Spada[4], F. Tatiana Mendoza[5], Claudia M. Barberis[5], Carlos Vay[5], M. Elena Arabolaza[6], Bibiana Paoli[6] and Eloísa I. Arana[1,3]**

[1] Institute of Immunology, Genetics and Metabolism (INIGEM), Clinical Hospital 'José de San Martín', University of Buenos Aires (UBA), National Council for Scientific and Technological Research (CONICET), Buenos Aires, Argentina, [2] Allergy and Immunology Division, Clinical Hospital 'José de San Martín', UBA, Buenos Aires, Argentina, [3] Department of Immunology, School of Medicine, UBA, Buenos Aires, Argentina, [4] Department of Pathology, Clinical Hospital 'José de San Martín', Buenos Aires, Argentina, [5] Department of Clinical Biochemistry and Bacteriology, School of Pharmacy and Biochemistry, Clinical Hospital 'Jose de San Martín', UBA, Buenos Aires, Argentina, [6] Pediatric Otolaryngology Division, Clinical Hospital 'José de San Martín', Buenos Aires, Argentina

Immune responses at the boundary between the host and the world beyond are complex and mucosal tissue homeostasis relies on them. Obstructive sleep apnea (OSA) is a syndrome suffered by children with hypertrophied tonsils. We have previously demonstrated that these tonsils present a defective regulatory B cell (Breg) compartment. Here, we extend those findings by uncovering the crucial role of resident pro-inflammatory B and T cells in sustaining tonsillar hypertrophy and hyperplasia by producing TNFα and IL17, respectively, in *ex vivo* cultures. Additionally, we detected prominent levels of expression of CD1d by tonsillar stratified as well as reticular epithelium, which have not previously been reported. Furthermore, we evidenced the hypertrophy of germinal centers (GC) and the general hyperplasia of B lymphocytes within the tissue and the lumen of the crypts. Of note, such B cells resulted mainly $(IgG/IgM)^+$ cells, with some IgA^+ cells located marginally in the follicles. Finally, by combining bacterial culture from the tonsillar core and subsequent identification of the respective isolates, we determined the most prevalent species within the cohort of OSA patients. Although the isolated species are considered normal oropharyngeal commensals in children, we confirmed their capacity to breach the epithelial barrier. Our work sheds light on the pathological mechanism underlying OSA, highlighting the relevance taken by the host immune system when defining infection versus colonization, and opening alternatives of treatment.

Keywords: tonsils, oral bacteria, obstructive, sleep, apnea, mucosal immunity

OPEN ACCESS

Edited by:
Nicolas Dutzan, University of Chile, Chile

Reviewed by:
Tetsuhiro Kajikawa, University of Pennsylvania, United States
Carla Alvarez Rivas, The Forsyth Institute, United States
Gustavo Andrés Monasterio, Karolinska Institutet, Sweden

****Correspondence:***
Eloísa I. Arana
eloarana@yahoo.com

Specialty section:
This article was submitted to Mucosal Immunity, a section of the journal Frontiers in Immunology

Received: *31 December 2020*
Accepted: *06 April 2021*
Published: *29 April 2021*

Citation:
Sarmiento Varón L, De Rosa J, Rodriguez R, Fernández PM, Billordo LA, Baz P, Beccaglia G, Spada N, Mendoza FT, Barberis CM, Vay C, Arabolaza ME, Paoli B and Arana EI (2021) Role of Tonsillar Chronic Inflammation and Commensal Bacteria in the Pathogenesis of Pediatric OSA. Front. Immunol. 12:648064. doi: 10.3389/fimmu.2021.648064

INTRODUCTION

Human paired palatine tonsils are lymphoid epithelial tissues of the oral mucosa around the oropharynx. They are part of the Waldeyer's ring of lymphoid tissue, which also comprise the adenoids and the lingual tonsils. The palatine tonsils (tonsils, from now on) are strategically located to generate mucosal immunity as they are constantly exposed to dietary and airborne antigens (Ags). Moreover, they have evolved for direct transport of foreign material from the exterior to the lymphoid cells through deep and branched crypts and the absence of Ag-degrading digestive enzymes (1). The surfaces of the human body, including the oropharynx, are colonized by several microbes, mainly bacteria, that establish a mutualistic relationship with the host. Tonsils are predominantly B-cell organs, immunologically most active between 4 and 10 years old. Some children (also some adults, but were not included in this study) present tonsillar hyperplasia and hypertrophy for yet unknown reasons. Such enlargement is the major pathophysiological sign underlying OSA, a highly prevalent disease, recognized as a major public health burden. OSA is characterized by repeated events of partial or complete upper airway obstruction during sleep that lead to disruption of normal ventilation with all the consequences implied due to hypoxemia. An increment in pro-inflammatory cytokines have been reported in blood from OSA patients (2–4). It is assumed that the B cell hyperplasia and hypertrophy that cause OSA are the result of chronic inflammation of palatine tonsils in children.

B cells contribute to immune responses during infectious, inflammatory and autoimmune diseases. In the last two decades, we have learned that B cells are able to modulate physiological and pathological processes not only by producing antibodies (Abs) and presenting Ags but also by producing cytokines. It has been shown that B cells can occur in the form of several cytokine-secreting subsets with either pro- or anti-inflammatory functions (5). Being an important reservoir of human B cells, the tonsils serve as a platform to study such subsets. Within this framework, we have recently demonstrated that OSA tonsils rendered significantly lower percentages of interleukin 10 (IL10) producing B cells (Bregs) than tonsils excised due to recurrent tonsillitis, showing that Bregs have a more complex and interesting role in tonsillar disease than was hitherto appreciated. Moreover, such defect in Breg population correlated with an increment in the proportion of germinal center (GC) cells. This correlation reveals a role for the Breg subset in controlling GC reactions, as it is by means of GC cells that tonsils are hypertrophied (6). GCs are the microanatomical sites within secondary lymphoid organs, critical for memory B and plasma cell generation. There are also many other cellular and molecular players involved in controlling GC activity. For instance, it has been long known that the pro-inflammatory cytokine tumor necrosis factor alpha (TNFα) is a required autocrine B-cell growth factor (7).

In the present paper, we found that tonsillar mononuclear cells (TMC) from OSA tonsils effectively exhibit a pro-inflammatory cytokine profile rapidly in culture. Interestingly, under certain stimulating conditions, B lymphocytes became one of the main cell populations driving TNFα levels in culture *ex vivo*. On the other hand, tonsillar interleukin 17 (IL17) was produced primarily by $CD4^+$ T cells. At tissue level, we discovered CD1d expression by tonsillar stratified as well as reticular epithelium and corroborated the persistent hypertrophy of GC and the concomitant hyperplasia of B lymphocytes, prevalently IgG/IgM positive $(IgG/IgM)^+$. We identified a number of bacterial species in the tonsillar core of patients with tonsillar hypertrophy, considered normal oropharyngeal commensals in children. However, we confirmed their presence beyond the epithelial boundaries by fluorescence *in situ* hybridization (FISH). Thus, our observations suggest that tonsillar hypertrophy is a multifaceted condition not associated to the presence of a particular microorganism but more likely to a failure of normal immune homeostatic mechanisms caused by the local loss of the capacity to discriminate between commensals and pathogens of the host. All in all, when such discrimination is lost, commensals become pathogens. Therefore, we support the notion that OSA in children is of infectious nature, clearly not associated to a single species.

MATERIALS AND METHODS

Isolation of cells

Primary human mononuclear cells were isolated from tonsils obtained from patients (total n=54 taking into account all experiments, the particular number of samples per experiment were detailed in the corresponding Figure legends) undergoing tonsillectomy due to OSA. TMC were prepared as follows. Briefly, tonsils were collected in phosphate buffered saline (PBS) buffer containing 50 μg ml^{-1} amphotericin B (Richet, BA, Arg). Tissues were chopped with a scalpel in IMDM medium (see below) and passed through a 70 μm-pore-size cell strainer (Falcon, Thermo Fisher, BA, Arg). TMC were purified by density gradient centrifugation with Ficoll-Hypaque (GE Healthcare, Uppsala, Sweden). The viability of primary cells, as determined by trypan blue exclusion was greater than 99% in all preparations. Informed consent was obtained from subjects before the study. The institutional ethics committee (Clinical Hospital, School of Medicine, Buenos Aires) approved the collection and use of clinical material, conformed to the provisions of the Declaration of Helsinki (as revised in Edinburgh 2000). Informed consent was obtained from all participants and/or their legal guardian/s. FACS experiments were performed with freshly isolated cells only.

Cell culture

TMC were cultured in IMDM medium (Life Technologies, CA, USA) containing 10% heat-inactivated fetal calf serum, 2mM L-glutamine, 100 U/ml penicillin, 100 μg/ml streptomycin, 20 mM 4-(2-hydroxyethyl)-1-piperazineethanesulfonic acid buffer (HEPES), 1 mM sodium pyruvate and 50 μM 2-mercaptoethanol (all from Invitrogen, CA, USA). Human IL2 (20 ng/ml; R&D Systems, MN, USA) and human IL4 (20 ng/ml; R&D Systems, MN, USA) were added immediately before experiments also as supplements. When indicated, human recombinant hCD40L (250 ng/ml; R&D Systems, MN, USA) and 25 μM CpG-ODN 2006 (InvivoGen, CA, USA) were used. Cells were cultured at

$1x10^6$ cells/ml either in 24-well culture plates (1ml) or 48-well culture plates (0.5ml).

Antibodies and fluorescence-activated cell sorting (FACS)

Fluorochrome conjugated mAbs specific for human CD3 (Pacific Blue, clone UCHT1), human CD20 (FITC, clone L27 and APC H7 clone 2H7), human CD4 (PerCP, clone SK3), human IL17A (APC, clone BL168), TNFα (PE, clone IT-5H2 and BV711, clone Mab11), and respective isotype control mAbs were purchased from BD Biosciences (CA, USA) and Biolegend (CA, USA). Fixable viability dyes used were either eFluor 780 (eBioscience, CA, USA), Zombie Green (Biolegend, CA, USA) or Zombie Aqua (Biolegend, CA, USA) depending on the staining scheme. To detect intracellular cytokines in cultured cells, the latter were stimulated with PMA/Ionomycin/Brefeldin A for the last 5 hs of culture. Then, they were incubated with Cytofix/Cytoperm (BD PharMingen, CA, USA) for 20 minutes (min) in the dark and washed with Perm/Wash solution (BD PharMingen, CA, USA). Following permeabilization, the cells were stained with the respective anti-cytokine mAb. Cells were acquired using FACSAria II (BD Biosciences, CA, USA) and analyzed with FlowJo software (Treestar, OR, USA). Single stained controls were used to set compensation parameters. Fluorescence minus one and isotype-matched Ab controls were used to set analysis gates.

Statistical analyses

The results were analyzed using GraphPad Prism 7.0 software (Graph Pad Inc, CA, USA). The normality of variable distribution was assessed by the Shapiro–Wilk test, the hypothesis of normality was accepted when $p > 0.05$. Once the hypothesis of normality was accepted, comparisons were performed using unpaired Student t test. When normality resulted rejected, a Mann-Whitney test was used. In both cases, the null hypothesis being that 2 populations do not differ.

Bacterial cultures

Tonsillar samples were cultured on Columbia agar containing 5% sheep blood and chocolate agar (Laboratorios Britania, Argentina) at 37°C with 5% CO2 for 24 to 48 h. Anaerobes were cultured onto Brucella agar supplemented with hemin and vitamin K under anaerobic conditions. All isolates were identified by MALDI-TOF MS. The isolates were identified by the direct colony on plate extraction method as previously described (8). Mass spectra were acquired using the MALDI-TOF MS spectrometer in a linear positive mode (Microflex, Bruker Daltonics). Mass spectra were analyzed in a m/z range of 2,000 to 20,000. The MALDI Biotyper library version 3.0 and MALDI Biotyper software version 3.1 were used for bacterial identification.

Immunofluorescence

Cryostat sections (5-10 μm thickness) of tonsils were fixed and stained with mouse anti-human CD1d (clone NOR3.2/13.17 Santa Cruz Biotechnology, CA, USA) followed by chicken anti-mouse IgG antibody AlexaFluor 488 (Thermo Fisher Scientific, BA, Arg). $(IgG/IgM)^+$ cells were detected by addition of goat anti-human IgM+IgG (H+L) $F(ab')_2$ (Jackson Immunoresearch, PA, USA) followed by donkey anti-goat IgG AlexaFluor 594 (Jackson Immunoresearch, PA, USA). IgA^+ cells were detected by addition of goat anti-human IgA $F(ab')_2$ (InVivoGen, CA, USA) followed by anti-goat IgG AlexaFluor 594 (Jackson Immunoresearch, PA, USA). Cell nuclei were visualized with 4,6-diamidino-2-phenylindole staining (DAPI, Thermo Fisher Scientific, BA, Arg). Finally, slides were rinsed with phosphate buffered saline, air dried, mounted in Vectashield (Vector Labs, CA, USA) and sealed with a glass coverslip. Samples were examined with a Nikon Eclipse Ti-E fluorescence microscope (Nikon instruments Inc, Tokyo, Japan). Corresponding isotype controls were always added (see **Supplementary Information**).

Bacterial localization and immunostaining

A solution of 0.5 mg/ml of lysozyme (Sigma Aldrich, Darmstadt, Germany) in 0.1 M Tris-HCl and 0.05 M Na2EDTA was added to the cryosections, followed by incubation at 37°C for 3 h. Fixed, permeabilized tonsillar sections were then incubated in a moist chamber for 4hs at 48°C in hybridization buffer [0.9 M NaCl, 20 mM Tris-HCl (pH 7.6), 0.01% sodium dodecyl sulfate, 30% formamide] containing either the universal probe EUB388 AlexaFluor 488 labeled probe or the negative control (nonsense) NONEUB388 AlexaFluor 546 (Thermo Fisher Scientific, BA, Arg). Stringent washing was performed by incubating the slide in washing buffer [20 mM Tris-HCl (pH 7.6), 0.01% sodium dodecyl sulfate, 112 mM NaCl] at 48°C for 15 min in a moist chamber a number of times, and subsequently rinsed with ddH2O for 5min. Finally, probed-hybridized tonsil cryosections were subjected to immunofluorescence staining as described above to determine the distribution of bacteria within the different tissue compartments. Images were acquired with a Nikon Eclipse Ti-E microscope (Nikon Instruments Inc., Tokyo, Japan) or an Olympus FV1000/IX81 confocal microscope (Olympus Corporation, Tokyo, Japan) using an oil-immersion objective (60X; numerical aperture, 1.42).

RESULTS

Characterization of TNFα Production by B Cells From Hypertrophied Tonsils

It is long established that B-cell–derived TNFα plays a crucial role in the development of follicular dendritic cells (FDCs) and B-cell follicles in spleen (9–11). TNFα and IL10 are cytokines with antagonistic actions. Interestingly, tonsils from OSA patients present a defective Breg compartment which correlates with higher proportion of GC B lymphocytes [BGC (6)], larger GC (12), and increased numbers of T follicular helper cells (Tfh) (13) than tonsils excised by other pathologies. Taking all into account, it would be expected that OSA tonsils exhibit a significant lymphocyte–derived TNFα compartment. We examined TNFα expression at the single cell level by FACS, upon TMC culture. A set of cultures was treated for 24 hs with IL2 and IL4 (IL2+IL4), which promote survival of all lymphocyte subsets through slight stimulation (14). Another set of cultures was supplemented for 24

hs and 48 hs with CpG and CD40L (in addition to IL2 and IL4, IL2+IL4+CD40L+CpG) to target stimulation towards B cells, aiming to assess specifically their capacity to contribute to the tonsillar pool of TNFα. Single cells were selected based on FSC-A vs FSC-H analysis (Singlets gate, **Figure 1A**). The cells that were already dead prior to permeabilization were excluded from the analysis through a fixable dead cell staining (Viable gate, **Figure 1A** and **Supplementary Figure 1**). In agreement with previous observations (14), elevated levels of cell death were linked to stimulation of tonsillar cultures (**Figures 1A, B**), dominated by a variety of terminally differentiated and highly activated B cells. In fact, we used this decay in the viability of the TMC cultures to monitor for suitable activation. In our experience, TMC culture stimulation is quite susceptible to minimal changes in experimental conditions (cellular density or FCS and activation cocktail batches, for instance). Therefore, when comparing cytokine secretion within a cohort of patients, those cultures that did not present such evolution in terms of viability, proportion of $CD3^+$ and $CD20^+$ populations and CD20 down-modulation (**Figure 1A**), were not considered. Also, $CD3^+$ cells served as an internal control for cytokine expression (**Figure 1C**). As expected, we observed that TMC from hypertrophied tonsils produced considerable amounts of TNFα when stimulated. At 24 hs post stimulation, approximately one third (29% ± SD 22%) of the cells from the IL2+IL4 stimulated cultures, expressed TNFα and that percentage reached ~40% (37%± SD 16%) in CD40L+CpG+IL2+IL4 stimulated cultures. The latter cultures were particularly affected by the surface CD20 down-modulation which takes place in response to general stimuli (15), albeit more pronounced with CD40L stimulation, as it has been extensively described previously (6, 16). Interestingly, B cells ($CD20^+$) expressing TNFα were those presenting lower levels of CD20 ($CD20^{down}$ $TNF\alpha^+$ cells, **Figure 1A**) suggesting that TNFα expression might be another functional consequence of CD20 modulation and the downstream signaling pathways triggered post internalization. These findings confirmed that the extent of CD20 down-regulation correlates with the degree of B cell activation (**Figures 1A, C**) (6, 15, 16). Despite the fact that lymphoid populations other than $CD20^+$ and $CD3^+$ cells in TMC are negligible (**Figure 1A**, non-cultured panel, double negative cells), their putative expansion, under the culture conditions used, needed to be tested as they would represent a putative contaminant of the $CD20^{down}$ cells. Tonsillar dendritic cells (tDC) identified as $CD20^-CD3^-CD11c^+$ appeared to increase their percentage within the $CD20^+CD20^{down}$ gate under stimuli. Even so, they represented 0.4%-0.7% of the latter, depending on the stimulus (**Supplementary Figure 2A**). Moreover, we could not detect any $CD11b^+$ cells among the cultured TMC (**Supplementary Figure 2B**). The proportion of innate lymphoid cells (ILC) was also assayed (**Supplementary Figure 3**) and proved to be negligible as well (detailed in the next section).

In order to compare TNFα expression by $CD20^{+/down}$ population with that of $CD3^+$ control cells within the same sample, we measured the median fluorescence intensity (MFI) for $TNF\alpha^+$ cells on both populations (**Supplementary Figure 4**). Regardless of the type and length of stimulation, average MFI for $CD3^+$ cells resulted around twice the same parameter for $CD20^{+/down}$ cells (**Figure 1D**). We next determined in which proportion $CD20^{+/down}$ and $CD3^+$ cells were contributing to the total $TNF\alpha^+$ population (**Figure 1E**). Comprehensibly, at 24 hs post stimulation with CD40L+CpG+IL2+IL4, when B cell activation peaked, $CD20^{+/down}$ cells represented the majority of tonsillar $TNF\alpha^+$ cells (52.4% ± SD 13.4% $CD20^{+/down}$ cells vs 41.7% ± SD 12.8% $CD3^+$ cells). On the other hand, at 48 hs post stimulation with CD40L+CpG+IL2+IL4, when tonsillar B cells showed strongly reduced viability, tonsillar $TNF\alpha^+$ population was dominated by $CD3^+$ cells (30.0% ± SD 11.7% $CD20^{+/down}$ cells vs 63.0% ± SD 15.9% $CD3^+$ cells). The cultures stimulated for 24 hs only with IL2+IL4 presented a tendency towards a slightly higher $CD20^{+/down}$ cells contribution to the $TNF\alpha^+$ cell pool than $CD3^+$ cells (**Figure 1F**). Importantly, the ability of tonsillar B cells to express TNFα was proved to be independent on the presence of the T cells in the TMC sample (**Supplementary Figure 5**). Finally, we also tried stimulating the TMC cultures using as a surrogate antigen F(ab′)2 goat antibodies specific for IgM and IgG (in addition to CD40L+IL2+IL4) (14), obtaining very similar results to those of CD40L+CpG+IL2+IL4 stimulation (data not shown). Kim et al. (17) have previously reported that upon culture, TMC from hypertrophied tonsils rendered higher levels of $TNF\alpha^+$ in the supernatant than TMC from children with recurrent tonsillitis. These results extend such findings, indicating that being exposed to various stimuli, B cell population can largely contribute to the TNFα pool, supporting (if not promoting) tonsillar inflammation.

Presence of Inflammatory T Cells Co-Expressing IL17 and TNFα in Hypertrophied Tonsils

It has been suggested that development of OSA is associated with peripheral Th17/Treg imbalance and is characterized by a pro-inflammatory cytokine microenvironment (2). We have previously reported on the ability of tonsillar B cells to secrete IL17 (6). However, while B cells as a population can dominate tonsillar TNFα production, we found IL17 secretion is indeed controlled by $CD3^+$ cells at every culture condition tested, including those specifically stimulating B lymphocytes (**Figures 2A, B**). TMC cultures supplemented with IL2+IL4 as well as those supplemented with CD40L+CpG+IL2+IL4 rendered an $IL17^+$ population which comprised ~ 90% $CD3^+CD4^+IL17^+$ cells at 24 and 48 hs. We confirmed this observation by measuring cytokines on the supernatant of some of the cultures by multiplex biomarker immunoassay (Luminex). We tried 4 different conditions to specifically stimulate B cells (CpG; CD40L; anti-(IgM/IgG)+CpG; anti-(IgM/IgG)+ CD40L), all of them in addition to IL2+IL4. We also added a culture treated only with IL2+IL4, as control. IL17 concentration did not significantly varied with culture condition compared to the control, as opposed to that of TNFα, which exhibited significant increments under B cell stimulating conditions (data not shown). As expected, $CD3^+IL17^+$ cells were confirmed to be $CD3^+CD4^+IL17^+$ (Th17) cells (**Figure 2B**). Moreover, we tried to estimate the putative contribution of cells other than Th17 and B

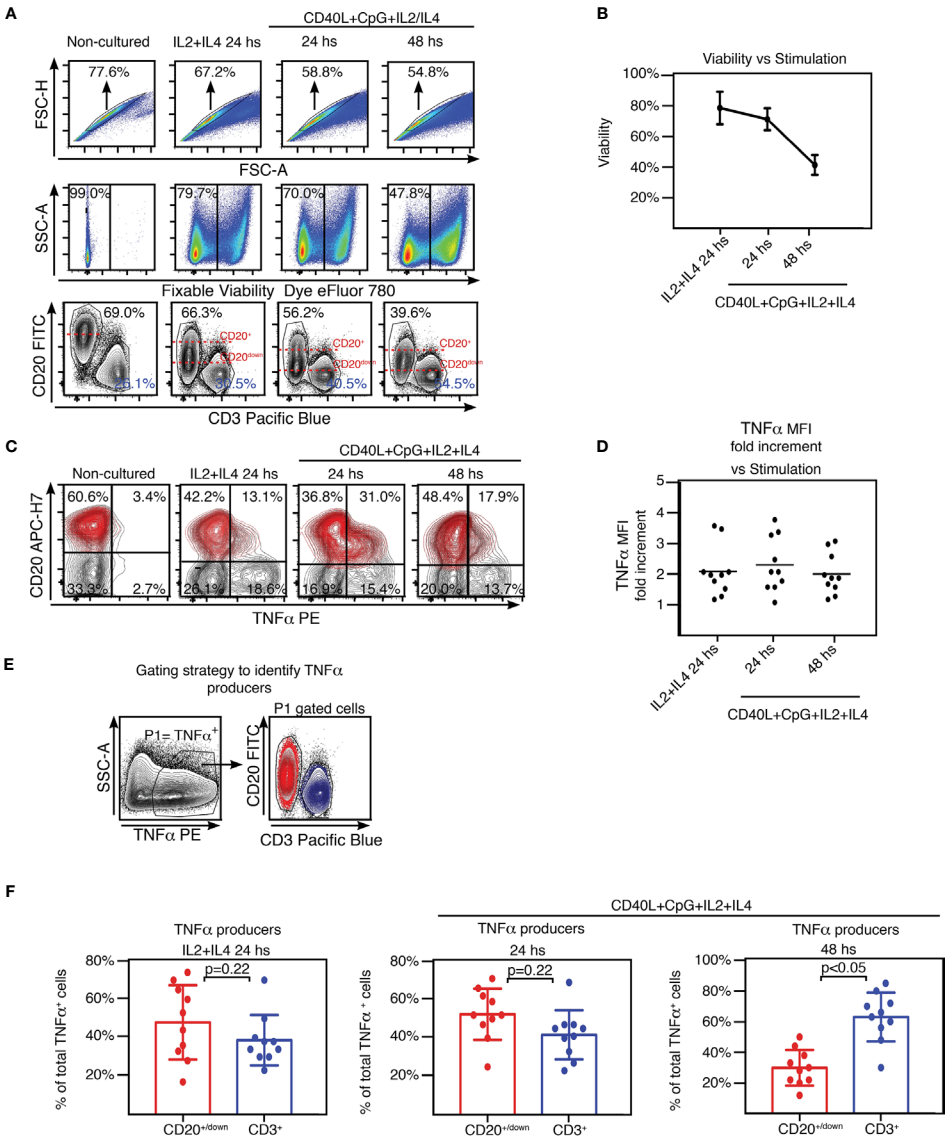

FIGURE 1 | TNFα expression by tonsillar mononuclear cells. **(A)** Freshly isolated TMC were cultured on IL2+IL4 alone or CpG+CD40L+IL2+IL4, for the time points indicated on the top of each panel. Non-cultured cells served as control (conserved at 4^0C). Cells were stained for surface CD20, CD3 and intracellular TNFα. Samples were subsequently analyzed by FACS. Gating strategy is partially illustrated. Singlets were gated by plotting FSC-H vs FSC-A for each sample (upper panels). Within the singlets population, dead cells were determined by a fixable viability dye. In this case, the viable gate corresponds to the eFluor 780^-cells (middle panels). Within the viable gate, lymphoid gate was determined through SSC-A vs FSC-A (not shown). Lower panels: CD20 vs CD3 contour plots. Percentages designate frequencies of the populations indicated. Dashed red lines show the decline of expression of CD20 post stimulation. Data from one experiment representative of 10 independent experiments performed with different individuals each one, are presented. Gates were manually adjusted due to the changes experienced by the cells in culture upon each treatment. **(B)** Line graph plotting the mean percentage ± SD of the frequencies of the viable gate pooled from the 10 independent experiments performed with stimulated TMC and detailed in **(A)**. **(C)** TMC were cultured under the same conditions and stained for the same molecules as in **(A)**. Gating strategy as in **(A)** (singlets-viable-lymphoid, not shown). Contour plots show TNFα and CD20 expression by TMC. Percentages designate frequencies of populations in each quadrant. $CD20^{+/down}$ cells appear highlighted in red, based on the gating performed on the corresponding CD20 vs CD3 graph as in **(A)**, using the backgating option, to exclude any CD3 contamination. Quadrants were manually adjusted due to the changes experienced by the cells in culture upon each treatment. Data from one experiment representative of 10 independent experiments performed with different individuals each one, are presented. **(D)** Graph showing the MFI fold increment=(TNFα MFI of $CD3^+TNFα^+$/TNFα MFI of $CD20^{+/down}$ $TNFα^+$) for each independent experiment at every stimulating condition. Calculations were made following FACS analysis depicted in **Supplementary Figure 4**. **(E)** Gating strategy used to estimate B and T cell specific contribution to the $TNFα^+$ cell pool from the 10 samples analyzed as shown in **(A–C)**. P1 denotes percentage of $TNFα^+$ cell population determined by TNFα vs SSC-A contour profile under the stimulations described above. Panel on the right, representative contour plots for CD20+/down (red) and $CD3^+$ (blue) populations within the P1 gate. **(F)** Histograms presenting the mean percentage ± SD of the $CD3^+$ and $CD20^{down/+}$ cell population frequencies from 10 independent experiments within the $TNFα^+$ cell pool for each stimulating condition, calculated as shown in **(E)** *p* value was calculated through unpaired *t* test, normality was confirmed by the Shapiro-Wilk test.

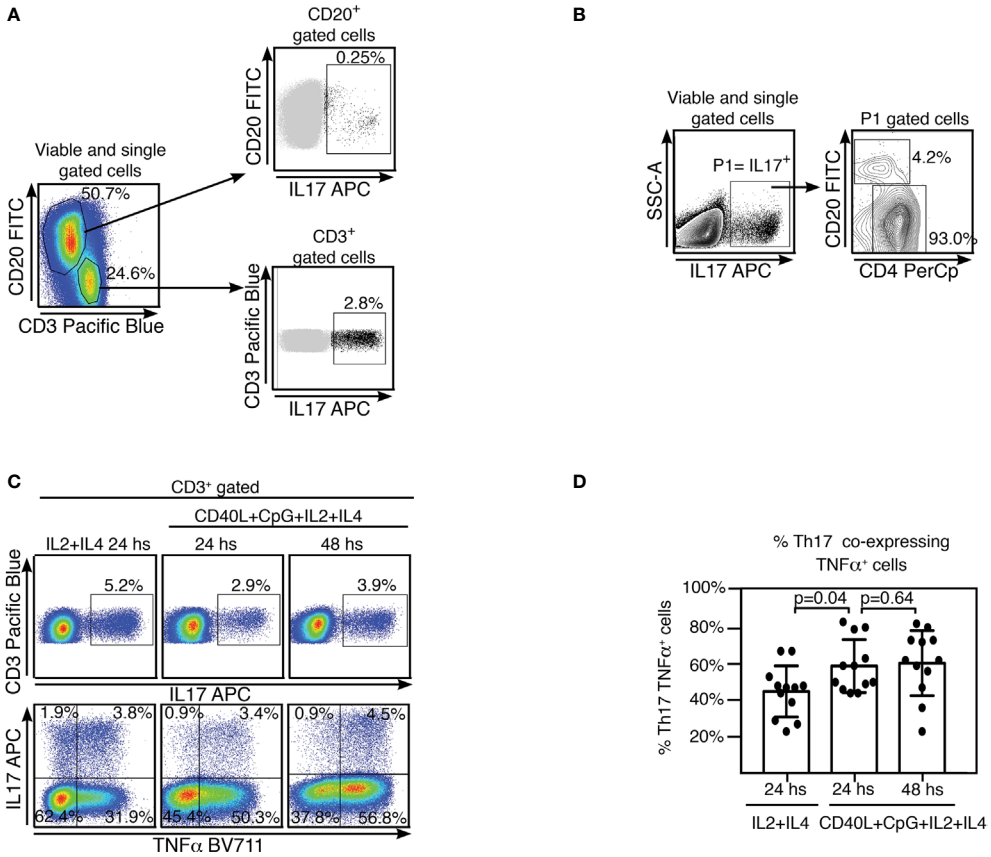

FIGURE 2 | Tonsillar Th17 cells co-express TNFα and IL17. **(A)** Freshly isolated TMC were cultured on CpG+CD40L+IL2+IL4 for 24 hs. Samples were subsequently analyzed by FACS. Gating strategy is partially illustrated. Singlets were gated by plotting FSC-A vs FSC-H for each sample (not shown). Within the singlets population, dead cells were determined by a fixable viability dye (see Methods). Within the viable gate, lymphoid gate was determined through SSC-A vs FSC-A (not shown). Cells were stained for surface CD20, CD3 and intracellular IL17. Pseudo-color plots show CD3 and CD20 expression by TMC upon stimulation, percentages designate frequencies of populations in each gate (left panel). Upper right panel: dot plot shows IL17 and CD20 expression by TMC, $CD20^+IL17^+$ population is highlighted in black and its frequency within $CD20^+$ population is indicated as percentage. Lower right panel: dot plot shows IL17 and CD3 expression by TMC, $CD3^+IL17^+$ population is highlighted in black and its frequency within $CD3^+$ population is indicated as percentage. Data from one experiment representative of 10 independent experiments performed with different individuals each one, are presented. **(B)** Gating strategy used to estimate the populations contributing to the $IL17^+$ cell subset upon stimulating strategy as in **(A)**. Singlets were gated by plotting FSC-A vs FSC-H for each sample (not shown). Within the singlets population, dead cells were determined by a fixable viability dye (see Methods). Within the viable gate, lymphoid gate was determined through SSC-A vs FSC-A (not shown). P1 denotes $IL17^+$ cell population determined by IL17 vs SSC-A contour profile. Panel on the right, representative contour plots for $CD20^+$ and $CD4^+$ populations within the P1 gate. Percentages designate frequencies of the populations indicated relative to P1 gate. Data from one experiment representative of 6 independent experiments performed with different individuals each one, are presented **(C)** Freshly isolated TMC were cultured on IL2+IL4 alone or CpG+CD40L+IL 2+IL4, for the time points indicated on the top of each panel. Singlets were gated by plotting FSC-A vs FSC-H for each sample (not shown). Within the singlets population, dead cells were determined by a fixable viability dye (see Methods). Within the viable gate, lymphoid gate was determined through SSC-A vs FSC-A (not shown). Cells were stained for surface CD20, CD3, intracellular TNFα and IL17 and finally analyzed by FACS. Upper panels: pseudo-color plots show IL17 vs CD3 expression by TMC. They correspond to events within singlets, viable, lymphoid and $CD3^+$ gates. Percentages designate frequencies of $IL17^+$ cells within $CD3^+$. Lower panels: pseudo-color plots show TNFα and IL17 expression by TMC, gated as in the upper panels. Percentages designate frequencies of populations in each quadrant, relative to the $CD3^+$ gate. Data from one experiment representative of 12 independent experiments performed with different individuals each one, are presented. **(D)** Histograms presenting the mean percentage ± SD of the Th17 $TNFα^+$ cell population frequencies from 12 independent experiments for each stimulating condition, calculated as shown in **(C)**, top right quadrant. *p* calculated through a Mann-Whitney test as the distribution of data in the middle column was not normally distributed.

lymphocytes, to the $IL17^+$ cell population pool. ILC3 are characterized by their capacity of secreting IL17 when stimulated. ILC3 represented around 0.03% of the TMC lymphoid gate (P3, **Supplementary Figure 3**). Their negligible fraction precluded us from detecting whether the culture conditions used stimulated them to express IL17. The same applied to Natural Killer (NK) cells which collectively signified 0.2% of the TMC lymphoid gate (P3, **Supplementary Figure 3**) but only a sub-fraction would be able to express IL17.

Th17 cells have appeared to exhibit plasticity of function and often co-produce other pro-inflammatory cytokines, particularly at sites of inflammation. Hence, we investigated whether tonsillar Th17 also expressed other cytokines as TNFα and interferon γ (IFNγ). The pseudo-color dot plots shown in **Figure 2C** were

gated on $CD3^+$ cells and show CD3 vs IL17 (upper panel) and IL17 vs TNFα (lower panel) staining. We detected co-expression of TNFα in a significant fraction of the Th17 cell population upon all culture conditions tested. At 24 hs post stimulation, nearly half of the Th17 population (44% ± SD 14%) from the IL2+IL4 stimulated cultures co-expressed TNFα. This percentage significantly increased when TMC were cultured with CD40L+CpG+IL2+IL4 for 24 hs (59% ± SD 14,5%) as well as for 48 hs (60%± SD 18%) indicating a positive correlation between higher frequencies of TNFα and IL17 and TNFα co-expression (**Figure 2D**). Low levels of expression of IFNγ observed upon the stimulating conditions tested precluded us from definitive conclusions regarding co-expression of IFNγ and IL17.

We concluded that tonsillar IL17 was produced primarily by Th17, which largely coproduced TNFα. Interestingly, several studies have linked the Th17 pathway with formation of GCs in mice spleens and ectopic B cell follicles at sites of inflammation (18–20). On the whole, TMC from hypertrophied tonsils promptly exhibited a pro-inflammatory cytokine profile in culture.

The Complex Histological Milieu of Tonsils and the Potential B Cell Contribution to Their Tissue Specific Inflammation

Like all mucosae, tonsillar immune actions (anti- and pro-inflammatory) must be tightly regulated, to balance the protection against virulent germs and the tolerance to harmless flora and innocuous Ags entering with air and food. Collectively, the results described above and others we have previously published (6, 14) are in agreement with the notion that tonsillar hypertrophy is a result of an imbalance between regulatory and effector immune functions which in turn lead to a local chronic inflammation. To this point, we have examined isolated cells. However, *in vivo*, immune processes occur in a complex tissue context which has to be comprehended. In order to recognize the histologic compartments within tonsils, we performed immune-fluorescence staining on cryosections from excised tonsils. The palatine tonsils are secondary lymphoid organs belonging to the mucosal associated lymphoid tissue (MALT), with unique histological characteristics. Unlike the lymph nodes, tonsils do not have afferent lymphatics, but present deep and branched crypts. Ag sample occurs through their distinctive tissue architecture and this is why tonsils are called lympho-epithelial organs. The tonsillar epithelium provides protection as well as serving to transport foreign material from the lumen to the lymphoid compartment. To evidence this mucosal surface, we tested the tonsillar epithelial cells' reactivity to antibodies against CD1d, since it has been reported its expression in other mucosal epithelial cells, like intestinal (21), epidermal keratinocytes (22) and vaginal epithelium (23). We confirmed CD1d expression in tonsillar epithelium. Anatomically, the surface epithelium of the palatine tonsils is an extension of the stratified squamous epithelium of the oral mucosa (**Figure 3A**, **Supplementary Figures 6, 7**). Importantly, in the crypts, the stratified epithelium becomes narrower and laxly textured [reticulated epithelium as termed by Oláh in 1978 (24)] and highly infiltrated with lymphocytes (**Figures 3B–D**). We observed CD1d expression in reticulated epithelium as well as in stratified squamous epithelium. Nevertheless, the level of that expression did not appear uniform at all levels of the multilayered squamous epithelium. The basal cells, which maintained an orientation perpendicular to the basement membrane, presented negligible immunoreactivity to anti CD1d. Conversely, CD1d was expressed strongly in the epithelial cells of the supra-basal and intermediate layers, significantly declining its expression in the apical layers. A similar pattern of CD1d staining is observed in the vaginal stratified epithelium (23). Expression was restrained mostly to the cell membrane in all cases (**Figure 3**). This epithelium was supported by a layer of connective tissue (**Figure 3A**) that separates it from the lymphoid component, and resulted negative for CD1d, with the exception of sporadic infiltrating lymphoid cells. **Figures 3B, C** show a region of crypts lined by reticulated epithelium. In fact, the crypt in **Figure 3C**, is lined by reticulated epithelium on one side and stratified squamous epithelium on the other. Two characteristics of the former are clear from the figures, and these are the desquamation of the upper cell layers and the absence or disruption of the basal layer of the epithelium. In this case, there is no boundary between the epithelium and the underlying lymphoid tissue. The cells in the intermediate layer were distorted and often separated from one another by the invading lymphoid cells, yet again CD1d exhibited high expression in this layer. The reticular epithelium trailed the curving shapes of the underlying follicles. To our knowledge, this is the first report on CD1d expression by tonsillar epithelium.

To visualize the lymphoid compartment, we stained for $(IgM/IgG)^+$ B cells (**Figure 3**). Our results confirmed previous reports (25). $(IgM/IgG)^+$ B cells (and plasma cells, distinguish by their size) appeared located not only in follicles, GC and their mantle zone, but also uniformly scattered throughout the tonsillar tissues (**Figures 3A–F**), generally associated in clusters when infiltrating reticular epithelial tissue (**Figure 3D**). IgA^+ B/plasma cells on the other hand, were mainly found outside the germinal centers, especially in the epithelium of crypts and rarely appear in the GCs (**Figure 3F**). Also, it can be observed the protrusion of lymphocytes and plasma cells from the sites of desquamation to the lumen (**Figures 3C, D**). IgG and IgM can be observed in its soluble form, accumulated on the apical surface of the epithelial layer (**Figures 3A, D**). It has been previously shown that nasopharyngeal epithelium widely expresses FcRn, which mediates IgG transport across the epithelial cell layer (26). On the other hand, it does not express pIgR, hence the transport of dimeric IgA is unfeasible through this kind of epithelia (27), making IgG the predominant protective isotype in tonsils. The histological findings we described above are in agreement with those reports. Moreover, FcRn and CD1d belong to the same family of proteins, the non-classical MHC class I molecules and both have been shown to display a restriction in their expression to specific tissues, namely epithelial cells from other mucosal sites (28). Finally, follicular hyperplasia was present in all samples as well as intensively active germinal centers (**Figure 4**). Such hyperplasia is attributable to proliferation of BGC, as we and others have previously shown (6, 12, 29). In light of the results shown in previous sections, such misguided

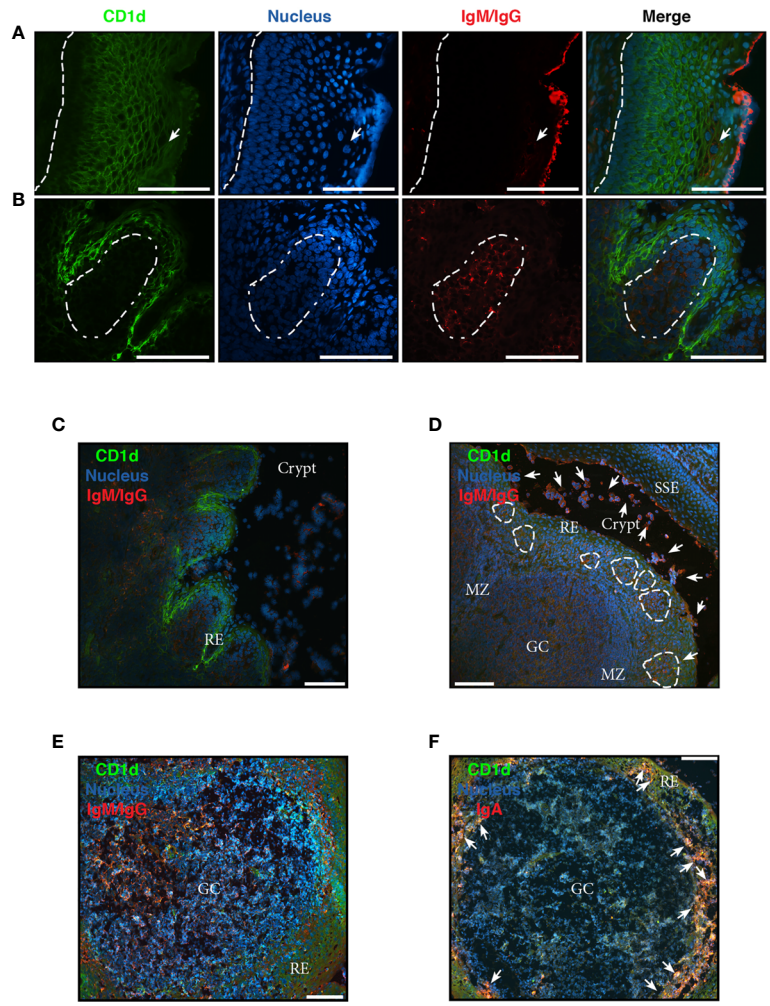

FIGURE 3 | Analysis of chronically inflamed human tonsils by immunohistology. **(A–F)** Three-color immunofluorescent microscopy of tonsillar frozen sections. **(A)** Representative immunofluorescence staining showing stratified squamous epithelium with CD1d (green), IgG/IgM (red) and nucleus (blue). Dashed line represents the limit between the basal membrane and the epithelium. Arrow indicates IgG^+/IgM^+ plasma and B cells intercalated in the mesh of epithelial cells. **(B)** Representative immunofluorescence staining showing reticular epithelium with CD1d (green), IgG/IgM (red) and nucleus (blue). Dashed lines represent the limit of the follicle. **(A, B)** Scale bar, 100 µm. **(C)** A less magnified image of the section shown in **(B)** to evidence the particular characteristics of the lympho-epithelium covering the crypts. RE stands for reticular epithelium. Scale bar, 100 µm. **(D)** Representative immunofluorescence staining showing a germinal center (GC) with its mantle zone (MZ), the reticular epithelium (RE) over it highly infiltrated with lymphocytes. Clusters of B/plasma cells indicated by dashed lines. The crypt and the stratified squamous epithelium (SSE) on the other border of the crypt are also designated in the picture. CD1d (green), IgG/IgM (red) and nucleus (blue) staining. Arrows indicate some of the many IgG^+/IgM^+ B and plasma cells scattered all over the tissue and crypt. Scale bar, 100 µm. **(E)** Representative immunofluorescence staining showing single a germinal center (GC). CD1d (green), IgG/IgM (red) and nucleus (blue) staining. Scale bar, 100 µm. **(F)** Representative immunofluorescence staining showing a single germinal center (GC). CD1d (green), IgA (red) and nucleus (blue). Arrows indicate some of the many IgA^+ B and plasma cells into the mesh of the reticulated epithelium (RE). Scale bar, 100 µm. Samples were examined with a Nikon Eclipse Ti-E microscope.

B cell response can potentially fuel the local inflammatory microenvironment, extending the impairment of immune homeostatic control.

Microbiological Aspects of Hypertrophied Tonsils

The most evident potential source of a local persistent immune response would be a local persistent infection. However, as opposed to recurrent tonsillitis, tonsillar hypertrophy has been long considered of non-infectious etiology. Actually, hypertrophied tonsils serve as non-infected control for tonsils affected by recurrent tonsillitis in a number of publications, including relevant and recent ones in which such control should be crucial (30). It has been generally considered that bacterial cultures from hypertrophied tonsils largely reflect oropharyngeal colonization. It is actually quite complex to distinguish infection versus colonization, provided that tonsils, being part of the mucosal immune system, are constantly exposed to the environment.

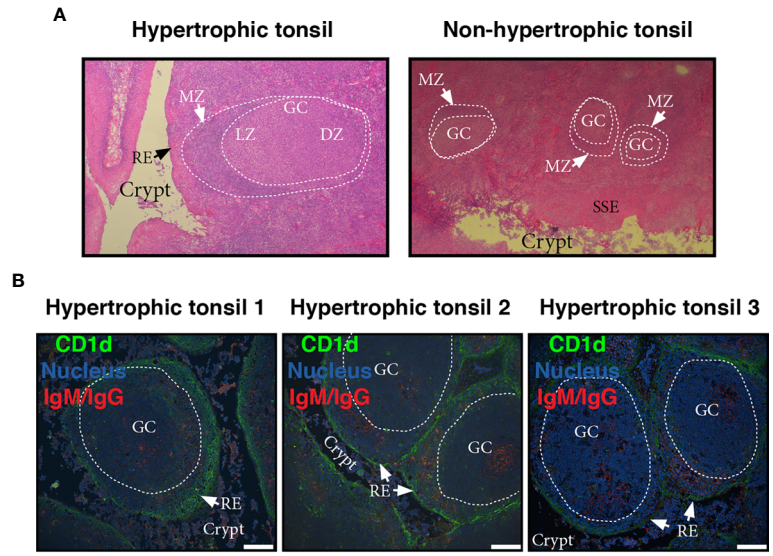

FIGURE 4 | Microscopic features of germinal centers from hypertrophic tonsils. **(A)** Comparative light microscopy of GC from an hypertrophic tonsil (left) and a non-hypertrophic tonsil (right) which evidence the difference in size largely documented in literature. H.E, original magnification 40x. MZ of the follicles is indicated by white arrows. LZ stands for light zone and DZ stands for dark zone. RE and SSE are also denoted in the pictures. **(B)** Three colour immunofluorescence staining showing GC from tonsils excised from three different OSA patients (1, 2, 3, see also colour code). Note the lymphoid hyperplasia, the degree of infiltration of the reticular epithelium (RE) in all cases, and the crypts invaded by lymphoid cells (most B and plasma cells according to staining). Scale bar, 100 µm. Samples were examined with a Nikon Eclipse Ti-E microscope.

In order to try to discriminate between commensals and pathogens we started by naming the bacterial species that we could retrieve alive from the core of the samples upon cauterization of the surface, trying to identify abundant, relentless and viable populations from the clinical tissue. We cultured the core tonsillar tissue of 44 children undergoing tonsillectomy due to OSA, whose ages ranged from 2 to 15 years old (**Table 1**). Within our cohort of patients, the frequency of tonsillectomy varied with the age, peaking at 5-6 years old (**Figure 5A**). All samples rendered viable bacterial cultures except for one. At phylum level, the tonsil cultures were dominated by *Firmicutes* (predominantly from the genera *Streptococcus* and *Staphylococcus* in that order), *Proteobacteria* (mostly from the genera *Neisseria* and *Haemophilus*), *Bacteroidetes* (principally genera *Prevotella*), *Actinobacteria* and *Fusobacterium* (**Tables 2** and **3**) in agreement with recent data obtained by next generation sequence (NGS) (31).

TABLE 1 | Basic demographic data of tonsils donors and number of viable bacteriological isolates produced by their samples.

Age group (years)	N° patients [a] (%) [b]	N° bacterial isolates [c]	Co-isolated bacteria [d]
2 -5	18 (41)	58	3,2 ± 1,5
6 -9	18 (41)	52	2,9 ± 1,3
10 -13	7 (16)	17	2,4± 1,0
14 -15	1 (2)	6	3,0 ± 1,4
Gender			
Males	27 (61)	80	3,0 ± 1,6
Females	17 (39)	53	3,1 ± 1,3

[a]*The values represent the number of patients in each group who donated samples after undergoing surgery due to obstructive sleep apnea (OSA). n=44 patients were analyzed, n=1 of them did not render viable bacterial cultures.*
[b]*The percentages were calculated relative to the total number of patients (n=44).*
[c]*Total number of bacterial isolates.*
[d]*Mean ±SD numbers of species co-infecting each individual in this cohort of patients per category of gender and age.*

Considering that certain microorganisms like *Streptococcus pyogenes (S. pyogenes), Streptococcus pneumoniae (S. pneumoniae), Moraxella catarrhalis (M. catarrhalis), Haemophilus influenzae (H. influenzae)* and *Staphylococcus aureus (S. aureus)* had been found either causing ear, nose and tonsil (ENT) pathology or as harmless local flora, both situations in competent hosts, we wanted to investigate their prevalence in our patients. We did not detect *M. catarrhalis* within our cohort of patients. We isolated *S. pneumoniae* from two patients. On the other hand, *S. aureus*, isolated from 45% of patients, accounted for the most frequent potentially pathogenic bacteria among the tonsils we analyzed, closely followed by *H. influenzae* (present in 27% of the patients) and *S. pyogenes* (on 23% of the samples). Bacterial isolates potentially pathogenic from the excised samples are shown in **Figure 5B**. In Argentina, vaccination against *H. influenzae* type b, *S. pneumoniae, Neisseria meningitidis (N. meningitidis)* and *Corynebacterium diphtheria*, which have been long known as commensal species in tonsils, is mandatory. We did not detect any patient carrying *Corynebacterium diphtheriae* but we found *Neisseria meningitidis* in the tonsils of a single patient and we did not serotype any isolate of *H. influenzae*.

In most cases we obtained co-isolates of different bacteria. Only 4 patients rendered cultures of single species, 3 of those

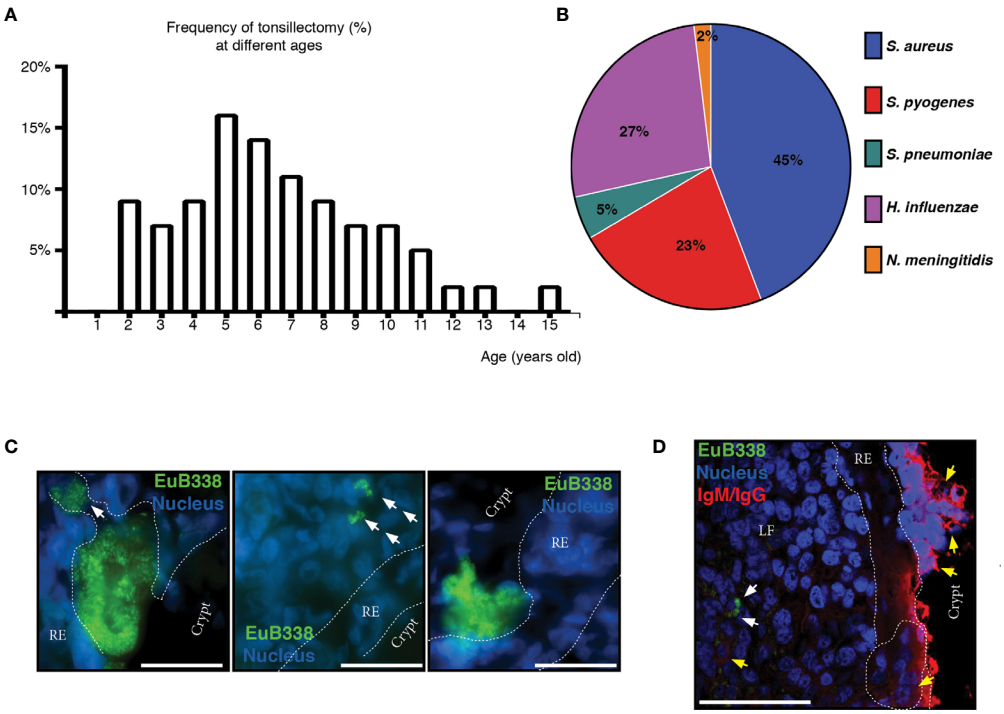

FIGURE 5 | Microbiological aspects of hypertrophic tonsils. **(A)** Age distribution of patients who had tonsillectomy due to OSA. **(B)** The graph shows the frequency of potential pathogenic bacterial detection in tonsils. **(C)** Microphotographs of the bacterial aggregates in tonsillar frozen sections from different OSA patients evidenced by fluorescence *in situ* hybridization (FISH) with a general eubacterial probe (EUB338-Alexa 488, green). Host cells nuclei were stained with DAPI (blue). Dashed line represents the limits of the reticular epithelium (RE) on both margins. White arrows indicate the conglomerates of bacteria that have penetrated the epithelial barrier. Scale bar, 50 µm. Samples were examined with a Nikon Eclipse Ti-E microscope. **(D)** Three-color immunofluorescent confocal microscopy of tonsillar frozen sections. Bacterial aggregates in tonsillar frozen sections were evidenced as in **(C)** and are indicated with white arrows. Yellow arrows indicate B and plasma cells. Dashed line represents the limits of the reticular epithelium (RE) on both margins. Clusters of B/plasma cells are enclosed by dashed lines. LF stands for Lymphoid Follicle. Scale bar, 50 µm. Samples were examined with an Olympus FV 1000 confocal microscope.

were *Streptococcus pyogenes* group A. Co-isolates ranged from 2 to 7 species. Details of the mean of species co-isolated from each child and all isolated organisms from the samples are listed in **Tables 1–3**. As we isolated a plethora of viable bacteria considered commensal and potential pathogenic as well, we were still unable to discriminate whether the tonsillar hypertrophy is of infectious nature.

The basic distinction between a pathogen and a commensal is that the first one displays aggressive tools for invasion. Usually this represents that such pathogen is able to penetrate the epithelial barriers. Therefore, we set out to detect bacterial presence in tonsillar biopsies by FISH, which allowed us to investigate its distribution and organization *in situ*. We used a fluorescent universal eubacterial (EUB338) probe followed by immune-fluorescence staining on cryosections from excised tonsils. As shown in **Figures 5C, D**, we detected bacterial aggregates not only associated with the surface of the epithelium but also within the lymphoid compartment, having breached the reticular epithelium. Therefore, while we cannot ascertain that the microorganisms detected *in situ* as well as through culture are the initiators of the ongoing inflammatory response, we did evidence that the chronification of the process must be certainly related to bacterial spreading beyond the normal boundaries. Also, such invasion is not associated to a single species as it can be observed in different patients harboring different colonizers, which have become pathogens, given the host´ requirement of the surgery to restore homeostasis.

DISCUSSION

Tonsils offer a useful model to study the interactions between the human mucosal immune system and the microbes that populates them at the epithelial level. Clinical material is not scarce, as tonsillectomy remains one of the most frequent pediatric surgeries carried out worldwide as a result of diagnosis with OSA. They rank among the secondary lymphatic organs, so every single developmental B cell subset is represented. In this study, initially we show that B cells as a population are able to produce TNFα at similar levels than those reached by T cell population, depending on the stimulating conditions. We have previously demonstrated B cell ability to rapidly produce other pro-inflammatory cytokines as IL6, IL8 and IL17 (6). Taken together, these results led us to conclude that B cell hyperplasia boost the pathological inflammatory processes and tissue alterations characteristic of OSA tonsils. Furthermore, we

TABLE 2 | Taxonomic breakdown of isolates from the core of hypertrophied tonsils at phylum level.

Phylum	N° species	N° bacterial isolates[a] (%)[b]
Firmicutes	16	65 (49)
Proteobacteria	13	39 (29)
Bacteroidetes	7	15 (11)
Actinobacteria	5	8 (6)
Fusobacterium	2	6 (5)
Total	43	133 (100)

[a]*The values represent the number of bacterial isolates from tonsils represented at phylum level.*
[b]*The percentages were calculated relative to the total number of isolates identified from the patient's samples.*

TABLE 3 | Taxonomic breakdown of viable bacterial isolates from the core of hypertrophied tonsils at genus and species level.

Aerobic bacterial isolates	N° patients[a] (%)[b]
Actinomyces odontolyticus	1 (2)
Actinomyces graevenitzii	1 (2)
Corynebacterium argentoratense	1 (2)
Escherichia coli	1 (2)
Gemella haemolysans	1 (2)
Haemophilus influenzae	12 (27)
Haemophilus parainfluenzae	1 (2)
Neisseria elongata	3 (7)
Neisseria flavescens	3 (7)
Neisseria macacae	1 (2)
Neisseria meningitidis	1 (2)
Neisseria perflava	1 (2)
Neisseria sicca	1 (2)
Neisseria spp.	2 (5)
Neisseria subflava	10 (23)
Rothia dentocariosa	1 (2)
Rothia mucilaginosa	4 (9)
Staphylococcus aureus	20 (45)
Staphylococcus intermedius	1 (2)
Streptococcus anginosus	4 (9)
Streptococcus constellatus	1 (2)
Streptococcus dysgalactiae	2 (5)
Streptococcus intermedius	1 (2)
Streptococcus mitis	3 (7)
Streptococcus parasanguinis	1 (2)
Streptococcus pneumoniae	2 (5)
Streptococcus pyogenes	10 (23)
Streptococcus salivarius	9 (20)
Streptococcus viridans	6 (14)
Aggregatibacter aphrophilus	2 (5)
Aggregatibacter segnis	1 (2)
Anerobic bacterial isolates	
Capnocytophaga sp.	1 (2)
Fusobacterium necrophorum	4 (9)
Fusobacterium nucleatum	2 (5)
Prevotella intermedia	5 (11)
Prevotella oris	3 (7)
Prevotella melaninogenica	1 (2)
Prevotella nanceiensis	3 (7)
Prevotella nigrescens	1 (2)
Prevotella spp.	1 (2)
Solobacterium moorei	1 (2)
Veillonella atypica	2 (5)
Veillonella parvula	1(2)

[a]*The values represent the number of patients that rendered the isolated designated in the column of the left.*
[b]*The percentages were calculated relative to the total number of patients (n=44).*

detected a relevant proportion of $CD3^+$ cells secreting IL17, even though we did not use culture conditions capable of specifically stimulating T cells. It has been previously reported that Th17/Treg ratio measured in PBMC is positively related to the severity of OSA and serum levels of C-reactive protein (2). Interestingly, there are a number of human diseases in which B cells contribute to the pathology through the acquisition of a pro-inflammatory cytokine profile and thereby supporting T cell–mediated inflammation (18–20, 32, 33).

While others have reported on the expression of CD1d in different mucosal epithelial cells (21–23), we are the first ones to report its expression by tonsillar stratified as well as reticular epithelium. CD1d is a non-polymorphic MHC class I-like antigen-presenting molecule, restricted to lipid Ag presentation to invariant natural killer T cells (*i*NKT) cells. CD1d-binding lipid Ags from tumors as well as commensal and pathogenic microorganisms have been well characterized by many authors including ourselves (34–37). Tissue specific functions of *i*NKT cells were recently reviewed in (38). Of note, CD1d-mediated Ag presentation by epithelial/parenchimal cells can shape the outcome of immune responses by regulating *i*NKT cells function. This has been demonstrated for the case of hepatocytes, which through CD1d-lipid presentation induce *i*NKT cell tolerance in the liver, protecting from hepatic inflammation. Whereas *i*NKT cells were confirmed to be present in tonsils (39), it remains unknown their specific function at this tissue. Provided we found abundant epithelial expression of CD1d, the diversity of the tonsillar microbiota and the constant contact with environmental Ags, we suggest *i*NKT cells might be functionally as relevant at this site as they are in the gut (40).

Another non-classical MHC class I molecule which has been shown to be expressed by tonsillar epithelial cells is the FcRn. Tonsillar epithelium has been classified as a type II mucosal surface (27). In fact, such definition would fit for the stratified squamous epithelium. The specialized epithelium that covers the tonsillar crypts is only found in that location and is called either reticular or lymphoepithelium. Neither the squamous nor the reticular epithelium express pIgR, but they do express FcRn (41). Hence, the major post switch protective Ig isotype translocated to the lumen from the tonsillar crypts is IgG. Of note, IgM and IgG are the best isotypes to activate complement. This capacity makes them particularly efficient but also more injurious to the host due to the inflammation associated with such effector immune function. Through anti (IgM/IgG) staining we evidenced the hypertrophic GCs, origin of the IgG locally produced (**Figures 4**, **5**). We also stained for IgA and confirmed that IgA^+ B cells were mainly found outside the germinal centers. Of note, it has been recently discovered in murine intestine a network of cellular interactions that drives IgM-to-IgA class switch recombination in extrafollicular B cells, compatible with the pattern we observed (42).

When studying the pathogenesis of OSA caused by hypertrophic tonsils, host immune response is only one side of the equation. The other side of it, is the microbiota populating the tonsillar mucosal surface. A diverse pool of bacteria comprising both commensal and pathogenic organisms have been isolated from OSA tonsils. In this study we worked with a

cohort of patients whose ages ranged between 2 and 15 years old. In agreement with previous reports from patients elsewhere (43), the frequency of tonsillectomies within that age limit peaked at 5-6 years old, which is coincident with the beginning of the transition from deciduous to permanent dentition for most children. Interestingly, it has been shown that such process implies the most striking change in the salivary microbiome of all ages, when considering children from birth until 18 years old (44). Choi et al. (45) recently demonstrated that the microbiome profiles of saliva and tonsils are largely similar both, in terms of diversity and composition, in children operated due to OSA. Given the location of tonsils at the back of the oral cavity, it was somehow expected the close relation between the two microbial groups. We could therefore speculate that the important changes in the bacterial species detected when starting to acquire permanent teeth might exert extra pressure on the tonsils of some children, being the draining immune sites first handling oral Ags. Again, probably a number of factors are responsible for the loss of homeostasis, including those of the microflora but also an altered host cell immune function.

In relation to the specific bacterial species identified by culture in our samples, they are much in agreement with other studies performed either by culture or, more recently, by employing 16S rRNA gene sequencing (**Tables 2**, **3**) (31, 45–48). In our experiments, *S. aureus* (45%), *H. influenzae* (27%), *N. subflava* (23%) and S. *Pyogenes* (23%) were the most prevalent bacterial species in the core of hypertrophied tonsillar tissue within our cohort of patients. They were followed by different species of the genus *Streptococcus* and *Neisseria*. Finally, among the anaerobic prevalent isolates, we found species of *Prevotella, Veionella* and *Fusobacterium.* As we have pointed out, all these microorganisms have been isolated from around the world, from tonsils excised due to OSA and also because of recurrent tonsillitis. Clearly, there are some differences depending on the vaccination schemes operating in different countries, which might impact in differences in the prevalence within tonsils' crypts of *S. Pneumoniae* or *N. meningitidis*, for example. However, in general, there is consensus that the bacterial species we have found are normal oropharyngeal commensals in children. A point of particular interest to discuss is whether this means that such commensal can never be injurious. Noticeable, complications in the host immune system would imply the redefinition of most commensals as pathogens. On the other hand, a change in the model of life of these bacterial communities would have the same result. In this context, we identified bacterial aggregates *in situ*. Bacteria can subsist either in planktonic or biofilm states. Planktonic cells are freely motile entities persisting in a liquid environment. In contrast, most of the bacterial species we named above (*Haemophilus, Sptaphylococcus, Streptococcus*) have long been known to have the capacity of forming biofilms. In biofilms, bacteria exist as sessile aggregates encased in a self-produced complex polysaccharide matrix attached to a surface (49). The establishment of biofilms is acknowledged as a virulence factor as it allows bacteria to better resist host immune responses. While we could detect extensive aggregates attached to the surface, we did not intend to particularly identify biofilms, as we did not have samples from normal tonsils to ascertain whether biofilm presence is exclusive of pathology or not. In any case, we detect bacterial penetration through the epithelial layer to the lymphoid compartment.

The obstacle entailed by the lack of healthy pediatric tonsils to use as control group or any other comparator sample constrains the conclusions of our study to some extent. The findings described here are limited to OSA tonsils. We do not have grounds either to rule out or to extrapolate them to any other experimental model or physiological situations.

To conclude, the data presented here shed light on the contribution of the B cell compartment to the inflammatory response in OSA tonsils and underscore the importance of the interplay between the host immune system and the commensal microorganisms able to switch from asymptomatic colonization to invasive disease.

DATA AVAILABILITY STATEMENT

The raw data supporting the conclusions of this article will be made available by the authors, without undue reservation.

ETHICS STATEMENT

The institutional ethics committee (Clinical Hospital,School of Medicine, Buenos Aires) approved the collection, and use of clinical material conformed to the provisions of the Declaration of Helsinki (as revised in Edinburgh 2000). Informed consent was obtained from all participants and/or their legal guardian/s. Written informed consent to participate in this study was provided by the participants' legal guardian/next of kin.

AUTHOR CONTRIBUTIONS

LS and JR processed all the samples used in this study, performed most of the experiments and analyzed the data. RR performed a number of experiments. LB and PB performed cell sorting and advised on design of FACS experiments. GB and NS performed cryosections and H&E stainings. LS, JR, PF and BP critically reviewed and edited the manuscript. MA and BP provided samples. CB, CV and FM performed the microbiologic culture and identification. EA supervised and designed research, analyzed the data and wrote the manuscript. All authors contributed to the article and approved the submitted version.

FUNDING

This research was funded by the following Argentinean governmental agencies: ANPCyT (BID PICT 2015-0113) and UBA (20720170100004BA), granted to EA. LS was the recipient of a CONICET postgraduate scholarship.

ACKNOWLEDGMENTS

We dedicate this work to the memory of Dr P. D. Ghiringhelli, a casualty of the pandemic, after collaborating in the design of an Argentinian SARS-Cov2 detection kit that contributed to the management of the crisis locally. Co-mentor of the last author of this paper more than 20 years ago, his passion for science and its direct applications became his legacy. We are grateful to Dr. Gastón Amable and Dr. M. Elisa Picco for their technical assistance with the immunofluorescence staining. We also thank Dr M. V Gentilini, Dr S. Laucella and Dr Ailén Natale who kindly supplied reagents when we needed them most. EA is indebted to Melina Fernández, Ivana Tellas, Belen Palmarocchi and Martina Guerrero, extensive to many other mums, for their support to this work through a quarantine with no schools. Their contribution to the science shown here has been invaluable. Finally, we are grateful to the anonymous patients and/or their parents that consent for the donation of samples for this research project.

SUPPLEMENTARY MATERIAL

The Supplementary Material for this article can be found online at: https://www.frontiersin.org/articles/10.3389/fimmu.2021.648064/full#supplementary-material

REFERENCES

1. Brandtzaeg P. Secretory Immunity With Special Reference to the Oral Cavity. *J Oral Microbiol* (2013) 5:20401. doi: 10.3402/jom.v5i0.20401
2. Ye J, Liu H, Zhang G, Li P, Wang Z, Huang S, et al. The Treg/Th17 Imbalance in Patients With Obstructive Sleep Apnoea Syndrome. *Mediators Inflammation* (2012) 2012:815308. doi: 10.1155/2012/815308
3. Huang YS, Guilleminault C, Hwang FM, Cheng C, Lin CH, Li HY, et al. Inflammatory Cytokines in Pediatric Obstructive Sleep Apnea. *Med (Baltimore)* (2016) 95(41):e4944. doi: 10.1097/md.0000000000004944
4. Kheirandish-Gozal L, Gozal D. Obstructive Sleep Apnea and Inflammation: Proof of Concept Based on Two Illustrative Cytokines. *Int J Mol Sci* (2019) 20 (3):459. doi: 10.3390/ijms20030459
5. Fillatreau S. B Cells and Their Cytokine Activities Implications in Human Diseases. *Clin Immunol (Orlando Fla)* (2018) 186:26–31. doi: 10.1016/j.clim.2017.07.020
6. Sarmiento Varon L, DR ,J, Machicote A, Billordo LA, Baz P, Fernández PM, et al. Characterization of Tonsillar IL10 Secreting B Cells and Their Role in the Pathophysiology of Tonsillar Hypertrophy. *Sci Rep* (2017) 7(1):11077. doi: 10.1038/s41598-017-09689-x
7. Boussiotis VA, Nadler LM, Strominger JL, Goldfeld AE. Tumor Necrosis Factor Alpha is an Autocrine Growth Factor for Normal Human B Cells. *Proc Natl Acad Sci USA* (1994) 91(15):7007–11. doi: 10.1073/pnas.91.15.7007
8. Theel ES, Schmitt BH, Hall L, Cunningham SA, Walchak RC, Patel R, et al. Formic Acid-Based Direct, on-Plate Testing of Yeast and Corynebacterium Species by Bruker Biotyper Matrix-Assisted Laser Desorption Ionization-Time of Flight Mass Spectrometry. *J Clin Microbiol* (2012) 50(9):3093–5. doi: 10.1128/jcm.01045-12
9. Fu Y-X, Chaplin DD. Development and Maturation of Secondary Lymphoid Tissues. *Annu Rev Immunol* (1999) 17(1):399–433. doi: 10.1146/annurev.immunol.17.1.399
10. Endres R, Alimzhanov MB, Plitz T, Fütterer A, Kosco-Vilbois MH, Nedospasov SA, et al. Mature Follicular Dendritic Cell Networks Depend on Expression of Lymphotoxin β Receptor by Radioresistant Stromal Cells and of Lymphotoxin β and Tumor Necrosis Factor by B Cells. *J Exp Med* (1999) 189(1):159–68. doi: 10.1084/jem.189.1.159
11. Gonzalez M, Mackay F, Browning JL, Kosco-Vilbois MH, Noelle RJ. The Sequential Role of Lymphotoxin and B Cells in the Development of Splenic Follicles. *J Exp Med* (1998) 187(7):997–1007. doi: 10.1084/jem.187.7.997
12. Reis LG, Almeida EC, da Silva JC, Pereira Gde A, Barbosa Vde F, Etchebehere RM. Tonsillar Hyperplasia and Recurrent Tonsillitis: Clinical-Histological Correlation. *Braz J Otorhinolaryngol* (2013) 79(5):603–8. doi: 10.5935/1808-8694.20130108
13. Yamashita K, Ichimiya S, Kamekura R, Nagaya T, Jitsukawa S, Matsumiya H, et al. Studies of Tonsils in Basic and Clinical Perspectives: From the Past to the Future. *Adv Otorhinolaryngol* (2016) 77:119–24. doi: 10.1159/000441902
14. Perez ME, Billordo LA, Baz P, Fainboim L, Arana E. Human Memory B Cells Isolated From Blood and Tonsils are Functionally Distinctive. *Immunol Cell Biol* (2014) 92(10):882–7. doi: 10.1038/icb.2014.59[doi
15. Valentine MA, Cotner T, Gaur L, Torres R, Clark EA. Expression of the Human B-cell Surface Protein CD20: Alteration by Phorbol 12-Myristate 13-Acetate. *Proc Natl Acad Sci* (1987) 84(22):8085–9. doi: 10.1073/pnas.84.22.8085
16. Anolik J, Looney RJ, Bottaro A, Sanz I, Young F. Down-Regulation of CD20 on B Cells Upon CD40 Activation. *Eur J Immunol* (2003) 33(9):2398–409. doi: 10.1002/eji.200323515
17. Kim J, Bhattacharjee R, Dayyat E, Snow AB, Kheirandish-Gozal L, Goldman JL, et al. Increased Cellular Proliferation and Inflammatory Cytokines in Tonsils Derived From Children With Obstructive Sleep Apnea. *Pediatr Res* (2009) 66(4):423–8. doi: 10.1203/PDR.0b013e3181b453e3
18. Ding Y, Li J, Wu Q, Yang P, Luo B, Xie S, et al. Il-17ra Is Essential for Optimal Localization of Follicular Th Cells in the Germinal Center Light Zone To Promote Autoantibody-Producing B Cells. *J Immunol* (2013) 191(4):1614. doi: 10.4049/jimmunol.1300479
19. Barbosa RR, Silva SP, Silva SL, Melo AC, Pedro E, Barbosa MP, et al. Primary B-cell Deficiencies Reveal a Link Between Human IL-17-producing Cd4 T-cell Homeostasis and B-cell Differentiation. *PloS One* (2011) 6(8):e22848. doi: 10.1371/journal.pone.0022848
20. Quinn JL, Kumar G, Agasing A, Ko RM, Axtell RC. Role of TFH Cells in Promoting T Helper 17-Induced Neuroinflammation. *Front Immunol* (2018) 9:382. doi: 10.3389/fimmu.2018.00382
21. Blumberg RS, Terhorst C, Bleicher P, McDermott FV, Allan CH, Landau SB, et al. Expression of a Nonpolymorphic MHC Class I-like Molecule, CD1D, by Human Intestinal Epithelial Cells. *J Immunol* (1991) 147(8):2518–24.
22. Bonish B, Jullien D, Dutronc Y, Huang BB, Modlin R, Spada FM, et al. Overexpression of CD1d by Keratinocytes in Psoriasis and CD1d-dependent IFN-Gamma Production by NK-T Cells. *J Immunol* (2000) 165(7):4076–85. doi: 10.4049/jimmunol.165.7.4076
23. Kawana K, Matsumoto J, Miura S, Shen L, Kawana Y, Nagamatsu T, et al. Expression of CD1d and Ligand-Induced Cytokine Production are Tissue Specific in Mucosal Epithelia of the Human Lower Reproductive Tract. *Infect Immun* (2008) 76(7):3011–8. doi: 10.1128/IAI.01672-07
24. Olah I, Glick B. The Number and Size of the Follicular Epithelium (FE) and Follicles in the Bursa of Fabricius. *Poult Sci* (1978) 57(5):1445–50. doi: 10.3382/ps.0571445
25. Bernstein JM, Baekkevold ES, Brandtzaeg P. Chapter 90 - Immunobiology of the Tonsils and Adenoids. In: J Mestecky, ME Lamm, JR McGhee, J Bienenstock, L Mayer, W Strober, editors. *Mucosal Immunology*, *3rd ed.* Burlington: Academic Press (2005). p. 1547–72.
26. Heidl S, Ellinger I, Niederberger V, Waltl EE, Fuchs R. Localization of the Human Neonatal Fc Receptor (FcRn) in Human Nasal Epithelium. *Protoplasma* (2016) 253(6):1557–64. doi: 10.1007/s00709-015-0918-y
27. Iwasaki A. Exploiting Mucosal Immunity for Antiviral Vaccines. *Annu Rev Immunol* (2016) 34:575–608. doi: 10.1146/annurev-immunol-032414-112315
28. Blumberg RS, van de Wal Y, Claypool S, Corazza N, Dickinson B, Nieuwenhuis E, et al. The Multiple Roles of Major Histocompatibility Complex class-I-like Molecules in Mucosal Immune Function. *Acta Odontol Scand* (2001) 59(3):139–44. doi: 10.1080/000163501750266729
29. Passàli D, Damiani V, Passàli GC, Passàli FM, Boccazzi A, Bellussi L. Structural and Immunological Characteristics of Chronically Inflamed Adenotonsillar Tissue in Childhood. *Clin Diagn Lab Immunol* (2004) 11 (6):1154–7. doi: 10.1128/cdli.11.6.1154-1157.2004

30. Dan JM, Havenar-Daughton C, Kendric K, Al-Kolla R, Kaushik K, Rosales SL, et al. Recurrent Group A Streptococcus Tonsillitis is an Immunosusceptibility Disease Involving Antibody Deficiency and Aberrant T(FH) Cells. *Sci Transl Med* (2019) 11(478):eaau3776. doi: 10.1126/scitranslmed.aau3776
31. Fagö-Olsen H, Dines LM, Sørensen CH, Jensen A. The Adenoids But Not the Palatine Tonsils Serve as a Reservoir for Bacteria Associated With Secretory Otitis Media in Small Children. *mSystems* (2019) 4(1):e00169–18. doi: 10.1128/mSystems.00169-18
32. DeFuria J, Belkina AC, Jagannathan-Bogdan M, Snyder-Cappione J, Carr JD, Nersesova YR, et al. B Cells Promote Inflammation in Obesity and Type 2 Diabetes Through Regulation of T-cell Function and an Inflammatory Cytokine Profile. Proc. *Natl Acad Sci USA* (2013) 110(13):5133–8. doi: 10.1073/pnas.1215840110
33. Zhu M, Belkina AC, DeFuria J, Carr JD, Van Dyke TE, Gyurko R, et al. B Cells Promote Obesity-Associated Periodontitis and Oral Pathogen-Associated Inflammation. *J Leukoc Biol* (2014) 96(2):349–57. doi: 10.1189/jlb.4A0214-095R
34. Gentilini M, P ,ME, Fernández PM, Fainboim L, Arana E. The Tumor Antigen N-Glycolyl-GM3 is a Human CD1d Ligand Capable of Mediating B Cell and Natural Killer T Cell Interaction. *Cancer Immunol Immunother* (2016) 65 (5):551–62. doi: 10.1007/s00262-016-1812-y
35. Brigl M. How Invariant Natural Killer T Cells Respond to Infection by Recognizingmicrobial or Endogenous Lipid Antigens. *Semin Immunol* (2010) 22(2):79–86. doi: 10.1016/j.smim.2009.10.006
36. Kinjo Y, Tupin E, Wu D, Fujio M, Garcia-Navarro R, Benhnia MR, et al. Natural Killer T Cells Recognize Diacylglycerol Antigens From Pathogenic Bacteria. *Nat Immunol* (2006) 7(9):978–86. doi: 10.1038/ni1380
37. De Libero G, Moran AP, Gober HJ, Rossy E, Shamshiev A, Chelnokova O, et al. Bacterial Infections Promote T Cell Recognition of Self-Glycolipids. *Immunity* (2005) 22(6):763–72. doi: 10.1016/j.immuni.2005.04.013
38. Crosby CM, Kronenberg M. Tissue-Specific Functions of Invariant Natural Killer T Cells. *Nat Rev Immunol* (2018) 18(9):559–74. doi: 10.1038/s41577-018-0034-2
39. Jimeno R, Lebrusant-Fernandez M, Margreitter C, Lucas B, Veerapen N, Kelly G, et al. Tissue-Specific Shaping of the TCR Repertoire and Antigen Specificity of iNKT Cells. *Elife* (2019) 8:e51663. doi: 10.7554/eLife.51663
40. Brailey PM, Lebrusant-Fernandez M, Barral P. NKT Cells and the Regulation of Intestinal Immunity: A Two-Way Street. *FEBS J* (2020) 287(9):1686–99. doi: 10.1111/febs.15238
41. Iwasaki A. Mucosal Dendritic Cells. *Annu Rev Immunol* (2007) 25:381–418. doi: 10.1146/annurev.immunol.25.022106.141634
42. Reboldi A, Arnon TI, Rodda LB, Atakilit A, Sheppard D, Cyster JG. Iga Production Requires B Cell Interaction With Subepithelial Dendritic Cells in Peyer's Patches. *Science* (2016) 352(6287):aaf4822. doi: 10.1126/science.aaf4822
43. Mattila PS, Tahkokallio O, Tarkkanen J, Pitkäniemi J, Karvonen M, Tuomilehto J. Causes of Tonsillar Disease and Frequency of Tonsillectomy Operations. Arch. *Otolaryngol Head Neck Surg* (2001) 127(1):37–44. doi: 10.1001/archotol.127.1.37
44. Crielaard W, Zaura E, Schuller AA, Huse SM, Montijn RC, Keijser BJ. Exploring the Oral Microbiota of Children At Various Developmental Stages of Their Dentition in the Relation to Their Oral Health. *BMC Med Genomics* (2011) 4:22. doi: 10.1186/1755-8794-4-22
45. Choi DH, Park J, Choi JK, Lee KE, Lee WH, Yang J, et al. Association Between the Microbiomes of Tonsil and Saliva Samples Isolated From Pediatric Patients Subjected to Tonsillectomy for the Treatment of Tonsillar Hyperplasia. *Exp Mol Med* (2020) 52(9):1564–73. doi: 10.1038/s12276-020-00487-6
46. Viciani E, Montagnani F, Tavarini S, Tordini G, Maccari S, Morandi M, et al. Paediatric Obstructive Sleep Apnoea Syndrome (OSAS) is Associated With Tonsil Colonisation by Streptococcus Pyogenes. *Sci Rep* (2016) 6:20609. doi: 10.1038/srep20609
47. Johnston J, Hoggard M, Biswas K, Astudillo-García C, Waldvogel-Thurlow S, Radcliff FJ, et al. The Bacterial Community and Local Lymphocyte Response are Markedly Different in Patients With Recurrent Tonsillitis Compared to Obstructive Sleep Apnoea. *Int J Pediatr Otorhinolaryngol* (2018) 113:281–8. doi: 10.1016/j.ijporl.2018.07.041
48. Jeong JH, Lee DW, Ryu RA, Lee YS, Lee SH, Kang JO, et al. Bacteriologic Comparison of Tonsil Core in Recurrent Tonsillitis and Tonsillar Hypertrophy. *Laryngoscope* (2007) 117(12):2146–51. doi: 10.1097/MLG.0b013e31814543c8
49. Chole RA, Faddis BT. Anatomical Evidence of Microbial Biofilms in Tonsillar Tissues: A Possible Mechanism to Explain Chronicity. *Arch Otolaryngol Head Neck Surg* (2003) 129(6):634–6. doi: 10.1001/archotol.129.6.634

Conflict of Interest: The authors declare that the research was conducted in the absence of any commercial or financial relationships that could be construed as a potential conflict of interest.